

# Method for determining the fast axis and phase retardation of a wave plate

Ming-Horng Chiu, Cheng-Der Chen, and Der-Chin Su

Institute of Electro-Optical Engineering, National Chiao Tung University, 1001 Ta-Hsueh Road, Hsin-Chu, Taiwan

Received October 6, 1995; revised manuscript received April 10, 1996; accepted April 26, 1996

Based on the heterodyne interferometric technique and the discrimination technique of using two light beams with different wavelengths, a novel method for identifying the fast axis of a wave plate and evaluating its phase retardation is presented. Some of the merits of the method, such as, a simple optical setup, high stability, better resolution, and easier operation, are presented, and the validity of the method is demonstrated. © 1996 Optical Society of America.

## 1. INTRODUCTION

A wave plate is a commonly used optical element in an optical metrological system.<sup>1-5</sup> The retardation error of a wave plate significantly influences the measurement results. Furthermore, for accurate optical alignments it is necessary to identify the fast axis of the wave plate. Some papers<sup>6,7</sup> have reported how to identify the fast axis, but these studies were done qualitatively without high resolution. There are also some papers<sup>7-14</sup> on how to evaluate the phase retardation of a wave plate. Although the procedures reported have high resolution, they are performed under the condition that the fast axis be located accurately in advance at a special azimuth angle.

In this paper a novel method is presented that can identify the fast axis of a wave plate and at the same time evaluate its phase retardation. The method is based on the heterodyne interferometric technique and the discriminative technique of using two light beams with different wavelengths. The phase difference, rather than optical intensity, is measured electrically, thus giving better resolution. The method has some advantages such as a simple optical setup, high stability because of its common path configuration, and easier operation.

## 2. PRINCIPLE

The schematic diagram of this method is shown in Fig. 1. A linearly polarized light at wavelength of  $\lambda_1$  or  $\lambda_2$  passing through an electro-optic (EO) modulator is incident on a beam splitter BS and is divided into two parts: The reflected light and the transmitted light. The reflected light passes through an analyzer  $AN_r$ , then enters a photodetector  $D_r$ . If the amplitude of light arriving at  $D_r$  is  $E_r$ , then the intensity measured by  $D_r$  is  $I_r = |E_r|^2$ , where  $I_r$  is the reference signal. The transmitted light passes through a tested wave plate  $W$  and an analyzer  $AN_t$  and is detected by another photodetector  $D_t$ . If the amplitude of light arriving at  $D_t$  is  $E_t$ , then the intensity measured is  $I_t = |E_t|^2$ , where  $I_t$  is the test signal.

### A. Intensities of the Reference Signal and the Test Signal

For convenience, the  $+z$  axis is chosen to be along the light propagation direction and the  $y$  axis to be along the vertical direction. Let the incident light be linearly polarized in the  $x$  direction, the fast axis of the EO modulator under an applied electric field be  $45^\circ$  (the technique for locating the EO modulator is written in Appendix A), and the fast axis of the tested wave plate  $W$  be  $\theta$  with respect to the  $x$  axis. The transmission axes of the two analyzers  $AN_r$  and  $AN_t$  are along the  $y$  axis. Then the Jones vector<sup>15</sup> of  $E_r$  is

$$\begin{aligned} \begin{pmatrix} E_{rx} \\ E_{ry} \end{pmatrix} &= \begin{bmatrix} 0 & 0 \\ 0 & 1 \end{bmatrix} \begin{bmatrix} \exp(i\psi_x) & 0 \\ 0 & \exp(i\psi_y) \end{bmatrix} \\ &\times \begin{bmatrix} \cos \frac{\Gamma}{2} & i \sin \frac{\Gamma}{2} \\ i \sin \frac{\Gamma}{2} & \cos \frac{\Gamma}{2} \end{bmatrix} \begin{pmatrix} 1 \\ 0 \end{pmatrix} \\ &= \begin{bmatrix} 0 \\ i \sin \frac{\Gamma}{2} \exp(i\psi_y) \end{bmatrix}, \end{aligned} \tag{1}$$

the intensity of the reference signal is

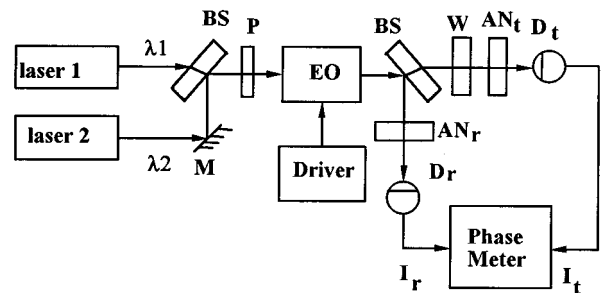


Fig. 1. Schematic diagram of the method: P, polarizer; BS, beam splitter; M, mirror; EO, electro-optic modulator; AN, analyzer; W, wave plate to be measured; D, photodetector.

$$I_r = |E_r|^2 = \frac{1}{2} (1 - \cos \Gamma), \quad (2)$$

where  $\Gamma$  is the phase retardation introduced by the electro-optic modulator and  $\psi_x$  and  $\psi_y$  are the phase shifts for the  $x$  component and the  $y$  component, respectively, of the reflected beam from BS. From Eq. (2) it is obvious that the intensity of the reference beam is independent of the phase shifts corresponding to the reflection from BS. In contrast, the Jones vector of  $E_t$  is

$$\begin{aligned} \begin{pmatrix} E_{tx} \\ E_{ty} \end{pmatrix} &= \begin{bmatrix} 0 & 0 \\ 0 & 1 \end{bmatrix} \begin{bmatrix} \cos \frac{\delta}{2} + i \sin \frac{\delta}{2} \cos 2\theta & i \sin \frac{\delta}{2} \sin 2\theta \\ i \sin \frac{\delta}{2} \sin 2\theta & \cos \frac{\delta}{2} - i \sin \frac{\delta}{2} \cos 2\theta \end{bmatrix} \begin{bmatrix} \cos \frac{\Gamma}{2} & i \sin \frac{\Gamma}{2} \\ i \sin \frac{\Gamma}{2} & \cos \frac{\Gamma}{2} \end{bmatrix} \begin{pmatrix} 1 \\ 0 \end{pmatrix} \\ &= \begin{bmatrix} 0 \\ i \sin 2\theta \sin \frac{\delta}{2} \cos \frac{\Gamma}{2} + i \cos \frac{\delta}{2} \sin \frac{\Gamma}{2} + \cos 2\theta \sin \frac{\delta}{2} \sin \frac{\Gamma}{2} \end{bmatrix}. \quad (3) \end{aligned}$$

Then the intensity of the test signal is

$$I_t = \frac{1}{2} [1 - \sqrt{A^2 + B^2} \cos(\Gamma + \phi)]; \quad (4)$$

where  $\delta$  is the phase retardation of  $W$  and

$$A = \cos^2 2\theta + \sin^2 2\theta \cos \delta, \quad (5)$$

$$B = \sin 2\theta \sin \delta. \quad (6)$$

In the above descriptions,  $\phi$  is the phase difference between  $I_t$  and  $I_r$ . It can be any value between 0 and  $2\pi$  with a period of  $2\pi$ ; here we arbitrarily define its value to be between  $-\pi$  and  $\pi$ . Then, according to the value of  $\delta$  and the signs of  $A$  and  $B$ ,  $\phi$  is given by the following expressions:

If  $0^\circ \leq |\delta| \leq 90^\circ$ , then

$$\phi = \tan^{-1}(B/A). \quad (7)$$

If  $90^\circ \leq |\delta| \leq 180^\circ$  and if

$$A \geq 0, \quad \text{then } \phi = \tan^{-1}(B/A); \quad (8)$$

$$A < 0 \text{ and } B \geq 0, \quad \text{then } \phi = \pi + \tan^{-1}(B/A); \quad (9)$$

$$A < 0 \text{ and } B < 0, \quad \text{then } \phi = -\pi + \tan^{-1}(B/A). \quad (10)$$

If  $\Gamma$  is constant, i.e., without the electro-optic modulator or with the electro-optic modulator off, then both  $I_r$  and  $I_t$  are constants, and it is difficult to evaluate the value of  $\phi$ . If a sawtooth voltage signal with amplitude  $V_{\lambda/2}$ , the half-wave voltage of the EO modulator, is applied to the EO modulator, then  $\Gamma = \omega t$ , where  $\omega$  is the angular frequency of the sawtooth signal. Thus from Eqs. (2) and (4) it is seen that the two detected output signals are sinusoidal with a phase difference  $\phi$ . These two sinusoidal signals are sent to a phase meter, and the phase difference  $\phi$  can be measured.

### B. Performing Procedures

From Eqs. (5)–(10) it is obvious that the phase difference  $\phi$  between  $I_t$  and  $I_r$  is a function of  $\theta$  and  $\delta$ . The relation

curves of  $\phi$  versus  $\theta$  for different  $\delta$  that are from  $-180^\circ$  to  $0^\circ$  and from  $0^\circ$  to  $180^\circ$  with an interval of  $30^\circ$  are shown in Figs. 2(a) and 2(b), respectively. It can be seen in these figures that, despite the values of  $\delta$ ,  $\phi$  equals zero when  $\theta$  equals  $0^\circ, 90^\circ, 180^\circ,$  and  $270^\circ$ . These values occur when  $I_t$  and  $I_r$  are in phase. So this behavior can be used for identifying the azimuth angle when  $\theta$  equals either  $0^\circ$  or  $90^\circ$ . Although the phase retardation of the wave plate at  $180^\circ$  or nearly  $180^\circ$  also has this behavior,

it is difficult to identify the azimuth angle when  $\theta$  equals either  $0^\circ$  or  $90^\circ$  by using only this behavior, because the curve of the phase difference is horizontal near  $\theta = 0^\circ$  and  $\theta = 90^\circ$ . Since the phase retardation of a wave

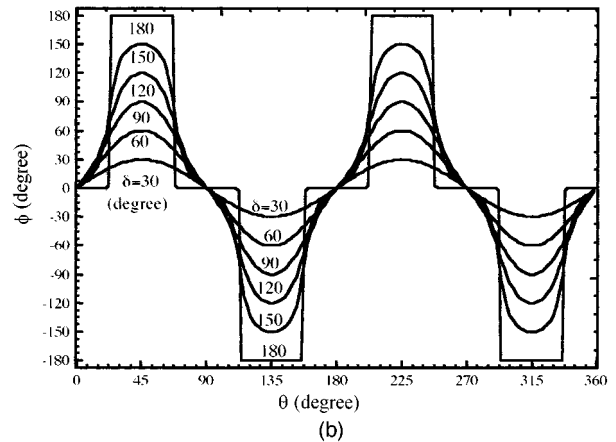
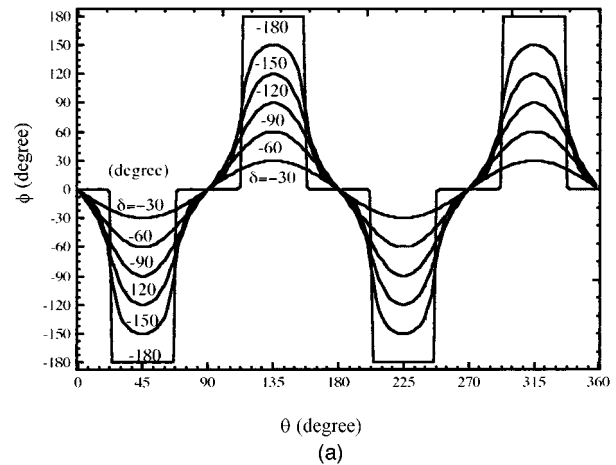


Fig. 2. Relation curves of  $\phi$  versus  $\theta$  for different  $\delta$ : (a)  $\delta = -180^\circ$  to  $0^\circ$ , (b)  $\delta = 0^\circ$  to  $180^\circ$ , at  $30^\circ$  intervals.

plate depends on the wavelength, we can solve this problem by introducing another light source of wavelength  $\lambda_2$ . Then the phase retardation of the wave plate is changed and  $\delta$  is no longer  $180^\circ$  or nearly  $180^\circ$ . Now the behavior can again be used to determine the azimuthal position at either  $\theta = 0^\circ$  or  $\theta = 90^\circ$ . In contrast,  $\phi$  has an extreme value when  $\theta$  equals  $45^\circ$ ,  $135^\circ$ ,  $225^\circ$ , and  $315^\circ$ . For  $\theta = 45^\circ$  and  $225^\circ$ ,  $\delta = \phi$ ; and for  $\theta = 135^\circ$  and  $315^\circ$ ,  $\delta = -\phi$ . Consequently, the phase retardation can be estimated. On the basis of the above descriptions, the procedures for determining the fast axis and the phase retardation of a wave plate, specified for wavelength  $\lambda_1$ , can be summarized as follows:

1. Rotate the wave plate W until  $I_t$  and  $I_r$  are in phase (i.e.,  $\phi = 0$ ) with light source of wavelength  $\lambda_1$ . Then rotate the wave plate back and forth slightly to check the sensitivity of  $\phi$  versus  $\theta$ . If it is sensitive, then keep the wave plate at the azimuth angle where  $\phi$  equals zero. If it is insensitive, introduce another light source of wavelength  $\lambda_2$  and rotate the wave plate until  $\phi$  becomes zero. At this condition the fast axis of the wave plate is located at either  $\theta = 0^\circ$  or  $\theta = 90^\circ$ . This represents the situation in which either the fast axis or the slow axis is along the  $x$  axis.

2. Next rotate the wave plate counterclockwise by  $45^\circ$ , and  $\theta$  becomes either  $45^\circ$  or  $135^\circ$ . Under this arrangement light sources of wavelengths  $\lambda_1$  and  $\lambda_2$  are used separately, and  $\phi_1$  and  $\phi_2$ , respectively, are obtained. Note that the phase retardation of a wave plate has a period of  $360^\circ$ ; hence the corresponding  $\phi_1$  and  $\phi_2$  should be modified so that they are within the range  $0^\circ$  to  $360^\circ$ . The measurable range of the phase meter is between  $-180^\circ$  and  $180^\circ$ ; hence for the required modification to be obtained, the measured values of  $\phi_1$  and  $\phi_2$  must remain unchanged if they are positive; otherwise,  $360^\circ$  should be added to the data whenever it is negative.

3. Following the measurements of  $\phi_1$  and  $\phi_2$  in procedure 2, if the modified values of  $\phi_1$  and  $\phi_2$  are nearly satisfied with the following reference equation,

$$\phi_2 \equiv \frac{\lambda_1}{\lambda_2} \phi_1, \quad (11)$$

then the fast axis is at  $45^\circ$  to the  $x$  axis (i.e.,  $\theta = 45^\circ$ ), and the phase retardation to be measured is the original value  $\phi_1$ . Otherwise, the slow axis is at  $45^\circ$  (i.e.,  $\theta = 135^\circ$ ) to the  $x$  axis, and the phase retardation  $\delta$  to be measured is the negative of the original value of  $\phi_1$ .

### 3. EXPERIMENTS AND RESULTS

To demonstrate the validity of this technique, a quarter-wave plate (WPQ-6328-4M) and a half-wave plate (WPQ-6328-2M) manufactured by Japan Sigma Koki Ltd., specified for a 632.8-nm wavelength, were tested. A He-Ne laser with a  $\lambda_1 = 632.8$ -nm and a He-Cd laser with  $\lambda_2 = 441.6$ -nm were used. An EO modulator (PC200/2) manufactured by Electro-Optics Developments Ltd., with half-wave voltage 170 V for 632.8-nm and 118.6 V for 441.6-nm wavelength, was used in this test. A sawtooth signal with frequency 2 kHz and amplitude  $V_{\lambda/2}$ , the half-

wave voltage of EO modulator, was applied to the EO modulator. For a quarter-wave plate it was easy to identify the azimuthal position where  $\theta$  equals either  $0^\circ$  or  $90^\circ$ , and  $\phi_1 = 89.3^\circ$  and  $\phi_2 = 128.85^\circ$  were obtained when light sources of  $\lambda_1$  and  $\lambda_2$ , respectively, were used. Since  $\phi_1$  and  $\phi_2$  satisfied Eq. (11), the fast axis was at  $\theta = 45^\circ$ , and its phase retardation was  $89.3^\circ$ . For the half-wave plate it was difficult to identify the azimuthal position where  $\theta$  equals either  $0^\circ$  or  $90^\circ$ ; the second light source of wavelength  $\lambda_2$  was used to identify it. Then  $\phi_1 = -179^\circ$  and  $\phi_2 = 102.3^\circ$  were obtained when light sources of  $\lambda_1$  and  $\lambda_2$ , respectively, were used. Because  $\phi_1$  is negative, it was modified to  $\phi_{1m} = 181^\circ$  according to procedure 2. Since the modified value  $\phi_{1m}$  and  $\phi_2$  did not satisfy Eq. (11), the fast axis of the half-wave plate was at  $\theta = 135^\circ$ , and its phase retardation was  $179^\circ$ .

To verify the correspondence between theory and experiments with this method, after the fast axes of these two wave-plates were determined, the phase differences  $\phi$  were measured at different azimuth angles  $\theta$ . The measurement results of the phase difference  $\phi$  versus the azimuth angle  $\theta$  are shown in Fig. 3. In this figure the solid curves and the dashed curves represent the theoretical values, and the symbols  $\circ$  and  $\Delta$  represent the measured values at wavelengths of 632.8 and 441.6 nm, respectively. The phase retardations at 632.8 nm can be read at  $\theta = 45^\circ$  to be  $89.3^\circ$  in Fig. 3(a) and  $179^\circ$  in Fig. 3(b). These results are in good accordance with the original

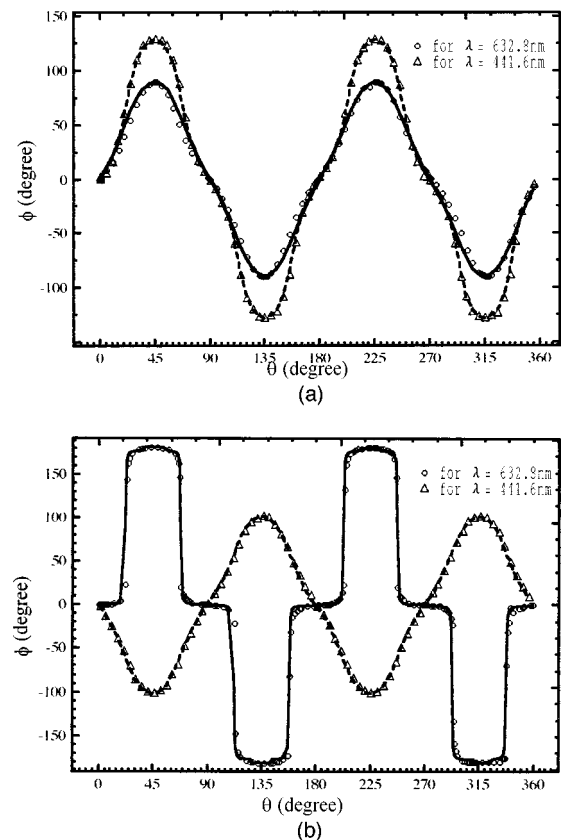


Fig. 3. Theoretical and experimental results for wave plates with 632.8-nm wavelength: (a) a quarter-wave plate, (b) a half-wave plate. Theoretical and experimental results with 441.6-nm wavelength are also included.

wave-plate specifications. The corresponding phase retardations at 441.6-nm wavelength are 128.85° and -102.3°.

#### 4. DISCUSSION

It is described in the beginning of Subsection 2.A that the precondition of this method is that the fast axis of the EO modulator be located accurately at 45° to the *x* axis. In the following, we discuss the influence of this accuracy on the determination of the fast axis and on the measurement of the phase retardation of the tested wave plate. If there is an azimuthal angular error  $\epsilon$  in locating the fast axis of the EO modulator, then the Jones matrix of the fast axis can be expressed as

EO

$$= \begin{bmatrix} \cos \frac{\Gamma}{2} - i \sin 2\epsilon \sin \frac{\Gamma}{2} & i \cos 2\epsilon \sin \frac{\Gamma}{2} \\ i \cos 2\epsilon \sin \frac{\Gamma}{2} & \cos \frac{\Gamma}{2} + i \sin 2\epsilon \sin \frac{\Gamma}{2} \end{bmatrix}. \quad (12)$$

With similar derivations from Eqs. (1)–(4), the intensities of the reference signal and the test signal are

$$I_r = \frac{\cos 2\epsilon}{2} (1 - \cos \omega t), \quad (13)$$

$$I_t = \frac{1}{2} (\gamma + \beta) - \frac{1}{2} [(\gamma - \beta \cos 2\alpha)^2 + (\beta \sin 2\alpha)^2]^{1/2} \cos(\omega t + \phi'), \quad (14)$$

respectively, where

$$\alpha = \tan^{-1} \left( \frac{\cos 2\epsilon \cos (\delta/2)}{\sin 2\theta \sin (\delta/2)} \right),$$

$$\beta = [\sin 2\theta \sin (\delta/2)]^2 + [\cos 2\epsilon \cos (\delta/2)]^2,$$

$$\gamma = \cos^2(2\theta - 2\epsilon) \sin^2 (\delta/2),$$

and

$$\phi' = \tan^{-1} \left\{ \frac{\cos 2\epsilon \sin 2\theta \sin \delta}{[\cos^2(2\theta - 2\epsilon) - \sin^2 2\theta] \sin^2(\delta/2) + \cos^2 2\epsilon \cos^2 (\delta/2)} \right\}.$$

According to Eqs. (13) and (14), the relation curves of  $\phi$  versus  $\theta$  for different  $\delta$  when  $\epsilon = 5^\circ$  and  $-5^\circ$  are shown in Figs. 4(a) and 4(b) respectively, in which the corresponding curves shown in Fig. 2 are added for comparison. In these figures, the solid and the dashed curves represent the results without and with azimuth angular error  $\epsilon$ , re-

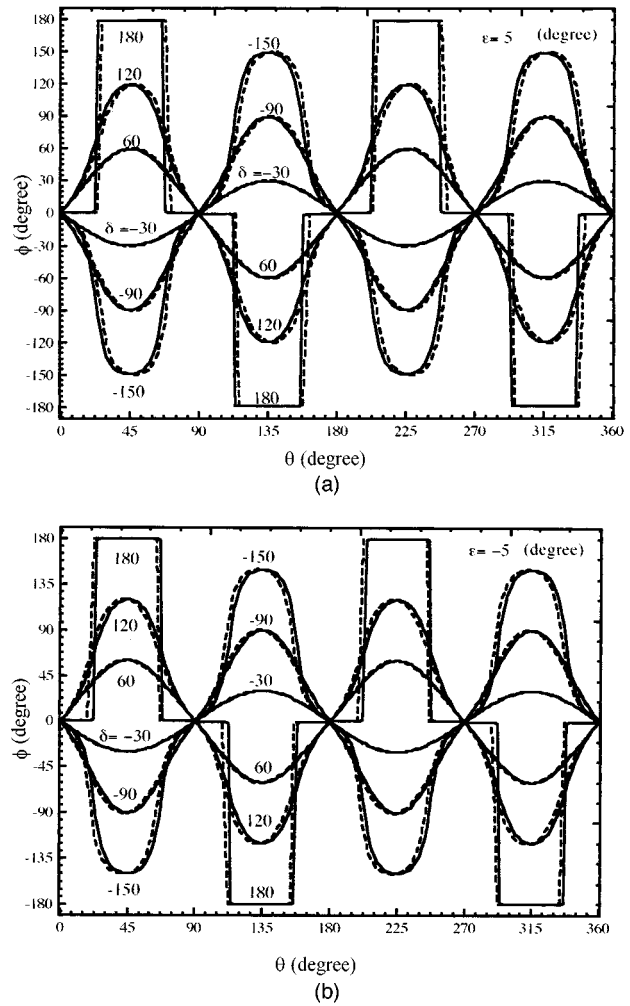


Fig. 4. Comparison of the relation curves of  $\phi$  versus  $\theta$  for different  $\delta$  as (a)  $\epsilon = 5^\circ$ , (b)  $\epsilon = -5^\circ$ . Solid and dashed curves represent results without and with azimuth angular error  $\epsilon$ , respectively.

spectively. Here, positive  $\epsilon$  means an error in the counterclockwise direction. It is seen that the behavior that  $\delta$  equals zero when  $\theta = 0^\circ, 90^\circ, 180^\circ$ , or  $270^\circ$  remains unchanged, so  $\delta$  has no influence on identifying the fast axis of the tested wave plate. In contrast, the measurement error of the phase retardation is

$$\Delta \delta = \tan^{-1} \left( \frac{\sin \delta}{\cos 2\epsilon \cos \delta} \right) - \delta. \quad (15)$$

With  $|\epsilon| = 2^\circ$  and  $5^\circ$ , the measurement errors of different wave plates are calculated and shown in Fig. 5. From these curves it is clear that even when  $|\epsilon|$  is as large as  $5^\circ$ ,

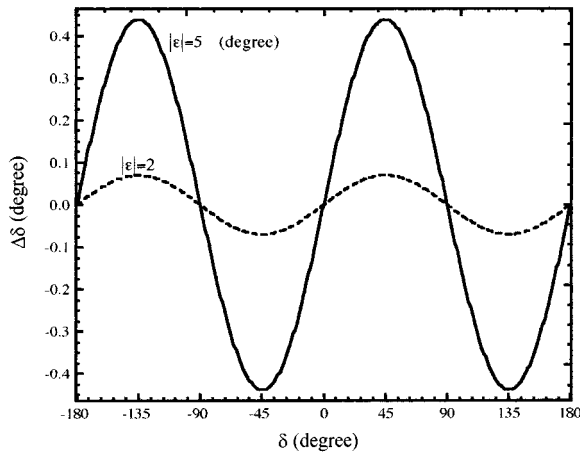


Fig. 5. Measurement errors for wave plates as  $|\epsilon| = 2^\circ$  and  $5^\circ$ .

the measurement error is still small. The maximum error occurs at the wave plates with phase retardations  $-135^\circ$ ,  $-45^\circ$ ,  $45^\circ$ , and  $135^\circ$ . However, the maximum error is always less than  $0.45^\circ$ .

This method is suitable for wave plates with phase retardation between  $0^\circ$  and  $360^\circ$ ; its resolution depends on the phase retardation of the wave plate and the resolution of the phase meter. Our experiments show that this method provides a resolution of better than  $0.1^\circ$  when a phase meter with  $0.01^\circ$  resolution is employed to measure a quarter-wave plate.

5. CONCLUSION

A novel method for identifying the fast axis of a wave plate and evaluating its phase retardation was presented. The method is based on the heterodyne interferometric technique and the discriminative technique of using two light beams with different wavelengths. Some of its merits are a simple optical setup, high stability, better resolution, and easier operation. The performance of this system was demonstrated.

APPENDIX A

In our experiments the fast axis of the EO modulator is located at  $\theta = 45^\circ$  by means of the following procedures:

1. The EO modulator is inserted between polarizer P and analyzer A as shown in Fig. 6, and we let the transmission axes of P and A be  $0^\circ$  and  $90^\circ$ , respectively, relative to the  $x$  axis. If the fast axis of the EO modulator is at  $\eta$  to the  $x$  axis and a sawtooth signal with angular frequency  $\omega$  and amplitude  $V_{\lambda/2}$  is applied to it, then the intensity detected by photodetector D can be expressed as

$$I = \frac{\sin^2 2\eta}{2} (1 - \cos \omega t), \tag{A1}$$

based on the derivations of Jones calculus. The signal is an ac signal with amplitude  $(\sin^2 2\eta)/2$ . It is obvious that the amplitude equals zero, and the signal becomes a dc signal when  $\eta = 0^\circ$  or  $90^\circ$  by rotation of the EO modula-

tor until a dc signal appears in the oscilloscope. Then the fast axis of the EO modulator is located at either  $\theta = 0^\circ$  or  $90^\circ$ .

2. The optical setup is modified, as shown in Fig. 7. The azimuth angle of the fast axis of the EO modulator is unchanged, and the transmission axes of the polarizer and the analyzers are located at  $45^\circ$  relative to the  $x$  axis. The incident beam is diffracted by acousto-optic modulator AOM and is divided into two beams of frequencies  $f_0$  and  $f_0 + f_s$ , where  $f_0$  is the optical frequency and  $f_s$  is the driven frequency applied to AOM. The beam of frequency  $f_0 + f_s$  is reflected by mirror M to polarization beam splitter PBS. Then  $x$ - and  $y$ -polarization components enter photodetectors  $D_1$  and  $D_2$ , respectively. The beam of frequency  $f_0$  passes through the EO modulator and also enters PBS. A sawtooth signal with frequency  $f$  and amplitude  $V_{\lambda/2}$  is applied to the EO modulator; thus the Jones vector of the light beam after leaving the EO modulator is

$$E_0 = \begin{Bmatrix} \exp\left[i2\pi\left(f_0 \pm \frac{f}{2}\right)t\right] \\ \exp\left[i2\pi\left(f_0 \mp \frac{f}{2}\right)t\right] \end{Bmatrix}, \tag{A2}$$

where the upper signs are taken if the fast axis of the EO is at  $\theta = 0^\circ$ . The beam is then divided by PBS, and the  $y$ - and the  $x$ -polarization components enter  $D_1$  and  $D_2$ , re-

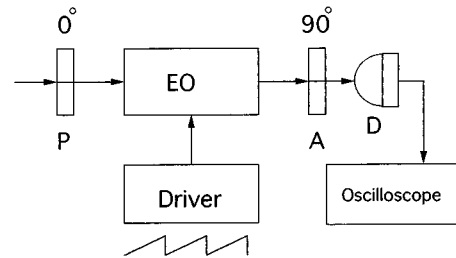


Fig. 6. Optical setup for locating the fast axis of the EO modulator at either  $\theta = 0^\circ$  or  $\theta = 90^\circ$ : P, polarizer; EO, electro-optic modulator; A, analyzer; D, photodetector.

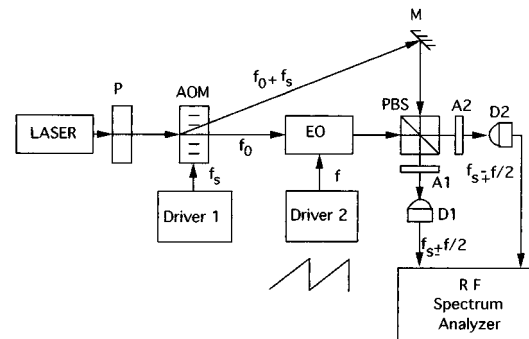


Fig. 7. Optical setup for identifying the fast axis of EO modulator: P, polarizer; AOM, acoustic-optic modulator; M, mirror; EO, electro-optic modulator; PBS, polarization beam splitter; A's, analyzer; D's, photodetectors.

spectively. Consequently,  $D_1$  and  $D_2$  detect the interference signals with beat frequencies at  $f_1$  and  $f_2$ , and they can be expressed as

$$f_1 = f_s \pm f/2, \quad (\text{A3})$$

and

$$f_2 = f_s \mp f/2, \quad (\text{A4})$$

respectively. These two signals are sent to the RF spectrum analyzer for comparison. If  $f_1 < f_2$ , the fast axis of the EO modulator is along the  $x$  axis (i.e.,  $\theta = 0^\circ$ ). Otherwise, the fast axis of the EO modulator is along the  $y$  axis (i.e.,  $\theta = 90^\circ$ ). After determining the fast axis of the EO modulator, we use a high-resolution rotation stage to rotate the fast axis of the EO modulator to  $\theta = 45^\circ$ .

## ACKNOWLEDGMENT

This study was supported by the National Science Council, Taiwan, under contract NSC 82-0417-E-009-346.

## REFERENCES

1. H. Takasaki, "Photoelectric measurement of polarized light by means of an ADP polarization modulator," *J. Opt. Soc. Am.* **51**, 461–462 (1961).
2. R. M. A. Azzam and N. M. Bashara, *Ellipsometry and Polarized Light* (North-Holland, Amsterdam, 1977), Chap. 5, p. 364.
3. P. S. Hauge and F. H. Dill, "Design and operation of ETA, an automated ellipsometer," *IBM J. Res. Dev.* **17**, 472–489 (1973).
4. D. C. Su and L. H. Shyu, "Phase shifting scatter plate interferometer using a polarization technique," *J. Mod. Opt.* **38**, 951–959 (1991).
5. P. Hariharan, "Double-pass interferometers," in *Optical Shop Testing*, D. Malacara, ed. (Wiley, New York, 1992), pp. 247–263.
6. G. Li, J. Li, and Y. Li, "Determination of the fast axis with an infrared spectrometer for quartz and mica waveplates," *Appl. Opt.* **29**, 1870–1871 (1990).
7. N. O'Flaherty, N. Kiyomoto, I. Shirahama, and Y. Mochida, "A system for high sensitivity measurement of birefringence using a photo-elastic modulator, and its applications," in *Electro-Optic and Magneto-Optic Materials II*, H. Dammann, ed., Proc. SPIE **1274**, 122–131 (1990).
8. B. R. Grunstra and H. B. Perkins, "A method for measurement of optical retardation angles near 90 degrees," *Appl. Opt.* **5**, 585–587 (1966).
9. C. M. McIntyre and S. E. Harris, "Achromatic wave plates for the visible spectrum," *J. Opt. Soc. Am.* **58**, 1575–1580 (1968).
10. Y. Lin, Z. Zhou, and R. Wang, "Optical heterodyne measurement of the phase retardation of a quarter-wave plate," *Opt. Lett.* **13**, 553–555 (1988).
11. E. Collett, "The measurement of the phase shift of a retarder," in *Polarized Light: Fundamentals and Applications* (Marcel Dekker, New York, 1993), pp. 130–138.
12. S. Nakadate, "High precision retardation measurement using phase detection of Young's fringes," *Appl. Opt.* **29**, 242–246 (1990).
13. M. Sypek, "A new technique for the measurement of phase retardation," *Opt. Laser Technol.* **23**, 42–44 (1991).
14. L.-H. Shyu, C.-L. Chen, and D.-C. Su, "Method for measuring the retardation of a wave plate," *Appl. Opt.* **32**, 4228–4230 (1993).
15. A. Yariv and P. Yeh, *Optical Waves in Crystals* (Wiley, New York, 1984), Chap. 5, pp. 121–131.